

A hybrid of fuzzy theory and quadratic function for estimating and refining transmission map

Jyun-Yu JHANG¹, Cheng-Jian LIN^{2,*}, Kuu-Young YOUNG¹, Chin-Teng LIN³

¹Institute of Electrical and Control Engineering, National Chiao Tung University, Hsinchu, Taiwan

²Department of Computer Science and Information Engineering, College of Electrical Engineering and Computer Science, National Chin-Yi University of Technology, Taichung, Taiwan

³Faculty of Engineering and Information Technology, University of Technology Sydney, Sydney, Australia

Received: 14.05.2018

Accepted/Published Online: 05.04.2019

Final Version: 18.09.2019

Abstract: In photographs captured in outdoor environments, particles in the air cause light attenuation and degrade image quality. This effect is especially obvious in hazy environments. In this study, a fuzzy theory is proposed to estimate the transmission map of a single image. To overcome the problem of oversaturation in dehazed images, a quadratic-function-based method is proposed to refine the transmission map. In addition, the color vector of the atmospheric light is estimated using the top 1% of the brightest light area. Finally, the dehazed image is reconstructed using the transmission map and the estimated atmospheric light. Experimental results demonstrate that the proposed hybrid method performs better than the other existing methods in terms of color oversaturation, visibility, and quantitative evaluation.

Key words: Dehazing, transmission map, fuzzy theory, quadratic function, image restoration

1. Introduction

Hazy images are obtained in several computer vision applications, such as terrain remote sensing, intelligent vehicles, target recognition, and tracking [1–4]. Such images are processed to obtain haze-free images, in which the actual scene and real color information are visible.

To improve the visibility and color fidelity of hazy images, many dehazing methods have been proposed [5–12]. These dehazing methods mainly follow two approaches: given depth [5, 6] and unknown depth [7–12]. In the given depth approach, depth information is added during image reconstruction. Tan and Oakley [5] used a forward-looking airborne camera to detect terrain height under different conditions and employed the obtained parameters as given depth information. By using a recaptured image, Narasimhan and Nayar [6] obtained given depth information by manually approximating the distance distribution of the sky area and the vanishing point. The vanishing point refers to a point on the image horizon at which parallel lines converge. Kopf et al. [7] used a three-dimensional geometric model to acquire given depth information. Because it is necessary to provide users with the equipment and given depth information for image reconstruction, this method is inappropriate for real applications.

The unknown depth approach is subdivided into multiple [8–12] and single [13–19] image processing. Schechner et al. [8, 9] used two or more images of a scene to estimate the depth of the scene at different degrees of polarization by rotating a polarizing filter. Narasimhan and Nayar [10–12] captured two or more images under

*Correspondence: cjlin@ncut.edu.tw

different haze conditions at the same scene and estimated the depth of a scene based on the haze concentration to reconstruct the image. According to the results reported in [8–12], the corresponding methods can be used to estimate depth information, but they cannot be used to obtain multiple images of the same scene.

Recently, dehazing using a single image [13–21] has been widely adopted to overcome the problem of multiple images. Fattal [13] assumed that transmission and surface colors are not correlated. On the basis of this assumption, he used independent component analysis to estimate the transmission of light and evaluate the real color of a scene from a Markov random field. However, this method cannot be applied to very hazy environments, and it requires considerable computation time and adequate color information. Tan [14] observed that haze-free images have higher contrast color than hazy images. To eliminate haze from an original image, Tan [14] proposed maximizing the local contrast of the recovered scene radiance. Although the method improves the contrast color of the output image considerably, color oversaturation occurs. Tarel and Hautiere [15] used the median filter to estimate the transmission map and adopted local adaptive smoothing and linear mapping for solving the halo problem. He et al. [16] proposed a dark channel method to estimate the transmission map of a hazy image and recover the image. First, the minimum pixel value of the three color channels of each pixel in an input image is extracted. Then, a predefined patch size is used to process the entire image, and the smallest pixel value in the patch is selected to replace the central value of the patch. Thus, the pixel value at the center of the patch becomes the gray value of one color channel. Then, the hazy and haze-free regions can be clearly distinguished in images, and the depth map of a hazy image can be estimated effectively. If a large patch size is used in [16], the halo phenomenon would usually occur for buildings, leaves, or pedestrians. In addition, if a small patch size is used in [16], colors in the reconstructed image would be oversaturated. This phenomenon is called color shift. To solve the halo problem, He et al. [16, 17] proposed the soft matting method and a guide filter to refine the transmission map and to filter the halo. The disadvantage of the method in [16, 17] is the increased computation time for image processing. Thus, many researchers have extended the dark channel method to overcome the halo and color oversaturation problems. Shiau [18] used the weight ratio between the pixels of an input image and the pixels of a patch to determine a threshold for solving the halo and color oversaturation problems. Huang et al. [4] used a small patch size to estimate the transmission map. They found that color shift occurred in one of the three color channels; that is, the pixel value of one color channel was especially high. On the basis of this observation in [4], they adjusted the proportions of three color channels to reconstruct images. Ancuti and Ancuti [19] presented the multiscale fusion concept to produce two images from a single image for dehazing a single image. By using the two images in conjunction with the scale-invariant feature transform method, multiple same images with multiple scales are generated. Then, each pixel generates three different weight values, namely luminance map, chromatic map, and saliency map. Finally, the reconstructed image is obtained by fusing the three different weight values. Wei et al. [20] used linear transformation to estimate the transmission map as well as to avoid the halo and color oversaturation problems. Wang et al. [21] proposed a fuzzy system to estimate the transmission map and used the weight ratio between the value of one pixel and the value of patch pixels to suppress the halo problem.

In the methods described in [4, 13–21], the color oversaturation problem is encountered. Therefore, in the present study, the focus is on single-image dehazing while solving the halo and color oversaturation problems. A fuzzy inference system and nonlinear compensation are employed for estimating the transmission map, whereas the color vector of atmospheric light is calculated using the mean value of the top 1% of the brightest light. Finally, the image is reconstructed using the estimated transmission map and the color vector of atmospheric light.

2. Background

The transmission of light is divided into two types. When light directly penetrates suspended particles in the air and is then introduced into the human eye or lens, it is said to be transmitted directly. In the environment, the distribution of suspended particles may be even or uneven. When light penetrates directly through a high density of suspended particles in the air, it will deviate from its original transmission path. This is called scattering. In the presence of few particles in the environment, a high-quality image can be obtained under clear sky or air. In contrast, in an environment with a high density of suspended particles, such as smoky or hazy environments, image quality will degrade.

In computer vision, this haze model [11–17] has been widely adopted, and it is expressed as follows:

$$I_c(x) = J_c(x) \times t(x) + A_c(1 - t(x)), \quad (1)$$

where I_c is a hazy image, and it represents the three RGB (red, green, and blue) color channels of each pixel; J_c represents a haze-free image; A_c is the color vector of atmospheric light; x is a pixel coordinate; $t(x)$ represents the transmission values of reflected light, and $t(x) \in [0, 1]$. $J_c(x) \times t(x)$ represents the direct attenuation or direct transmission of the scene radiance, and A_c is atmospheric light.

In general, atmospheric particles are assumed to be distributed evenly. According to the distribution conditions of atmospheric particles, the depth of the scene is attenuated exponentially when light penetrates through air. The transmission map $t(x)$ is formulated as follows:

$$t(x) = e^{-\beta d(x)}, \quad (2)$$

where the $d(x)$ is the depth value of an object at an environment position (x), and β denotes the attenuation coefficient. The transmission map is inversely proportional to the depth value.

Finally, the reconstructed image is derived from the haze model as follows:

$$J_c(x) = \frac{I_c(x) - A_c}{t(x)} + A_c. \quad (3)$$

3. Proposed dehazing method

In this section, an effective dehazing method is proposed for effectively eliminating halo and reconstructing a real color image. The proposed method consists of four steps and the haze image is shown in Figure 1a. Step 1 is based on the image depth of past observation to design a fuzzy inference system for estimating the transmission map. Image depth with haze is shown in Figure 1b. To overcome color oversaturation, a nonlinear quadratic function is used in Step 2 to refine the transmission map. In Step 3, a color vector of atmospheric light is picked by averaging the brightest 1% of the atmospheric light. The image is reconstructed in Step 4 by using the haze model. A flowchart of the proposed dehazing method is shown in Figure 2.

3.1. Transmission map estimation using fuzzy theory

Fuzzy logic was proposed by Zadeh [22] in 1968. It has been widely applied in various fields, such as control [23], image processing [24], and object recognition and identification [25]. A fuzzy inference system is shown in Figure 3. The fuzzifier transforms crisp data into suitable linguistic values. The fuzzy rule base contains the empirical knowledge of domain experts. The inference engine, which is the kernel of a fuzzy logic system, performs approximate reasoning. The defuzzifier is used to yield a crisp value from an inferred fuzzy value.



Figure 1. a) Haze image, b) image depth estimation.

The suspended particles of atmospheric is called transmission factor, which is a very important transmission medium for image. For example, haze is a natural phenomenon, in which dense suspended particles are aggregated. Variation in the degree of penetration or scattering of light depends on the number and distribution of particles. Because of the interaction between light and suspended particles, the real color of an image as it appears to the human eye or photographic equipment degrades owing to the variation distance. On the basis of physical phenomena, it is important to estimate the attenuation caused by particles. Under a known depth of scene and without photographic equipment, the relationship between a hazy image and a haze-free image can be observed in advance. Therefore, in this study, a fuzzy inference system is proposed to estimate the transmission map (Figure 4).

The RGB color values of each pixel are the input to a fuzzy inference system. The fuzzy set of each input variable is defined, as shown in Figure 5a, and the universe of discourse of each input is between 0 and 255. On the basis of the results of the plurality of experiments, a region with a lower pixel value in a hazy image has a higher saturation color (i.e. the region is a haze-free image area), and the intensity of the transmission map tends to 1. In the region with a middle pixel value (i.e. the region between the haze-free and hazy image areas), the intensity of the transmission map decreases as the pixel value increases. A region with a high pixel value represents a hazy or sky area. To avoid low saturation of the hazy region, the intensity of the transmission map is set to be close to zero. The fuzzy set of the transmission map intensity is defined as shown in Figure 5b. The centroid method is used for defuzzification. The output of the transmission map estimation is expressed as follows:

$$t(x) = \frac{\sum_{j=1}^R (\pi_{i=1}^N \mu_A(x_i)) \times y_j}{\sum_{j=1}^R (\pi_{i=1}^N \mu_A(x_i))}, \quad (4)$$

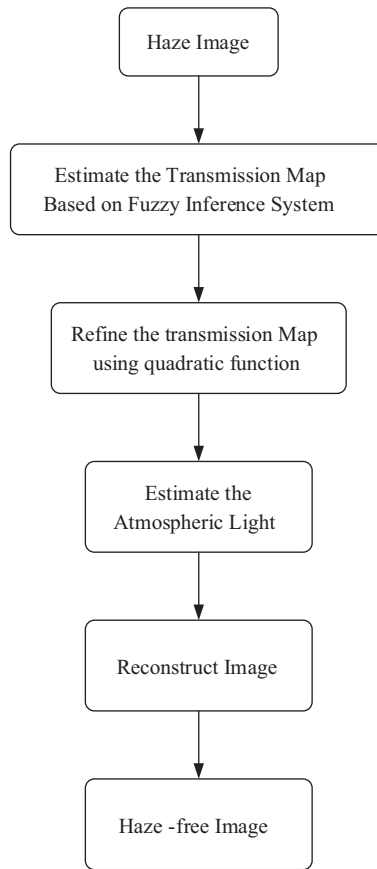


Figure 2. Flow diagram of the dehazing algorithm.

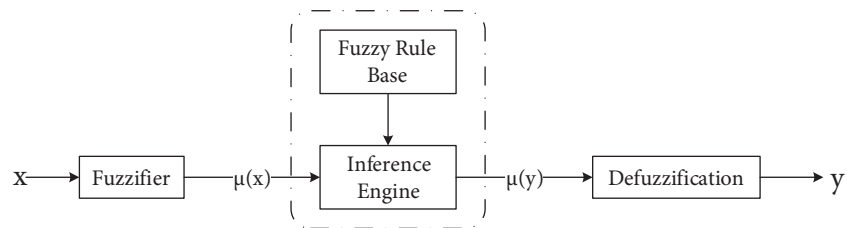


Figure 3. Block diagram of fuzzy inference system.

where N denotes the number of color channels, R represents the number of fuzzy rules, x_i represents the i th channel input, $\mu_A(x_i)$ represents the degree of membership value by which the i th channel input is excited, π represents the product operator, and y_j denotes the consequent part output of the transmission map. In this study, singleton values are used in the consequent part output.

Using three color channel pixels of the haze image in Figure 6a as the inputs to the fuzzy inference system for estimating the transmission map, a haze-free reconstructed image is obtained, as shown in Figure 6b. In this figure, color oversaturation is apparent. A low or high pixel value affects the estimation of the transmission map. Thus, a nonlinear curve is used to refine the transmission map.

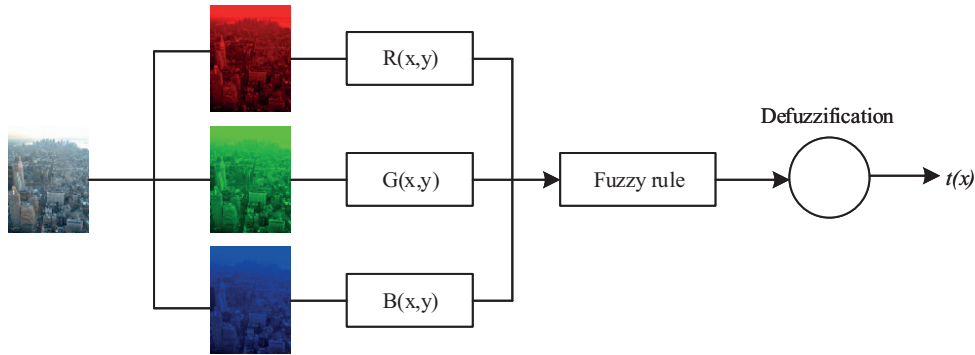


Figure 4. The transmission map estimation using a fuzzy inference system.

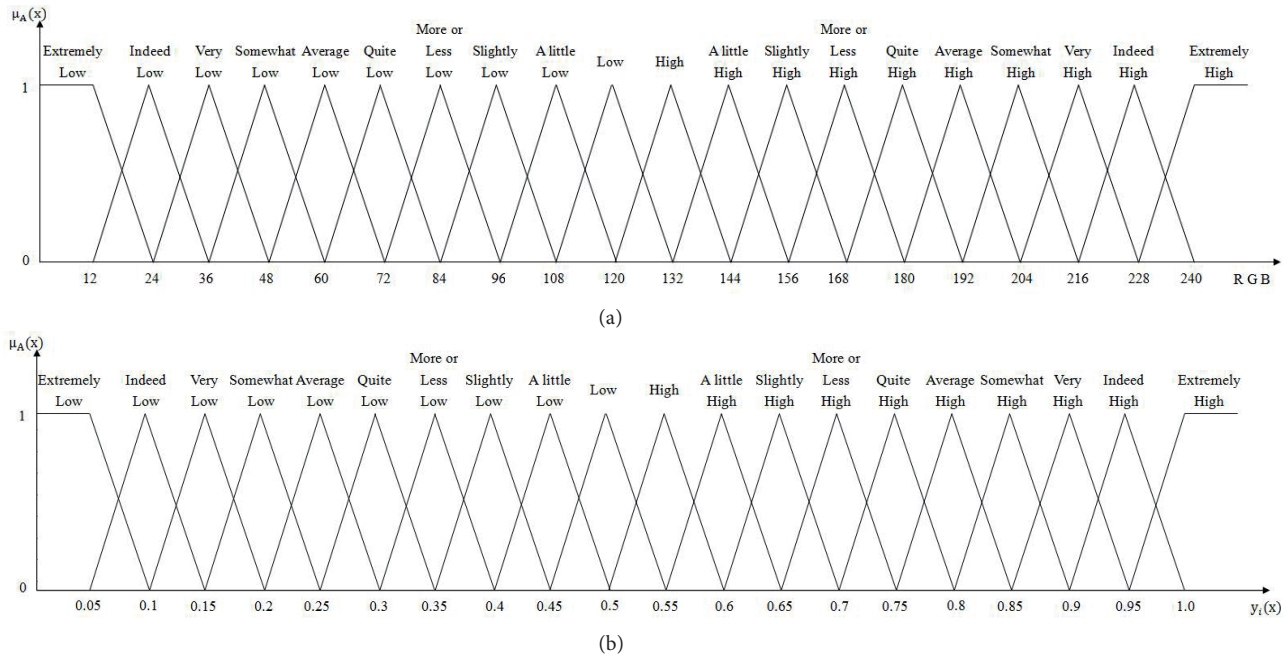


Figure 5. Membership function of a) antecedent part, b) consequence part.

3.2. Transmission map refinement using quadratic function

To solve the problem of color oversaturation, a quadratic function is proposed in this study to refine the transmission map, and it is expressed as follows:

$$t_{ref}(x) = f(t(x)) = a(t(x)^2) + b(t(x)) + \frac{p}{1+p}, \tag{5}$$

where $t(x)$ represents the transmission map estimated by the fuzzy inference system, coefficients a and b are constant values between -0.7 and 1.35 and are used to adjust the curve, and coefficient p represents the average gray value of the entire image for image compensation. According to the transmission map, the horizontal axis represents the reference transmission intensity between 0 and 1 , whereas the vertical axis represents the refining transmission intensity. As shown in Figure 7, when the transmission intensity is close to zero, the region represents the sky, a white object, or haze. Because few particles are usually present in the air on a sunny day, distant objects still appear hazy. Therefore, the term $\frac{p}{1+p}$ in Eq. (5) is adopted to refine the transmission



Figure 6. a) Haze image, b) haze-free image using transmission map estimation based on a fuzzy inference system.

map. In addition, the intensity of the transmission map of the region between the haze-free and hazy regions has a strong effect on image quality. The coefficients a and b are used to adjust the quadratic function. If the intensity of the transmission map is approximately the same as that of the linear transmission map, the problem of color oversaturation cannot be overcome. Conversely, if the intensity of the transmission map is large and is approximately the same as 1, the region is a haze-free area and therefore does not require dehazing.

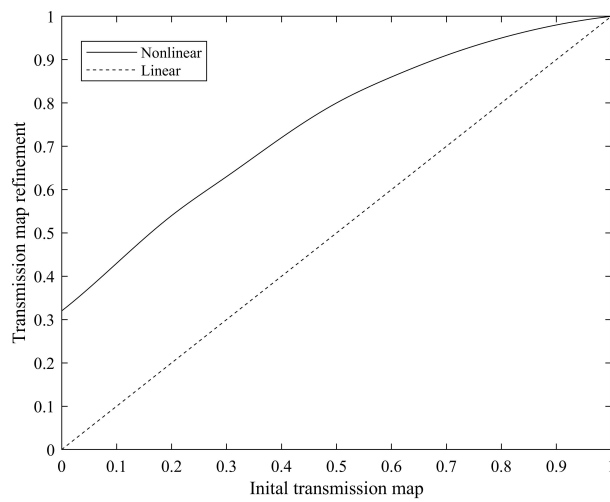


Figure 7. The transmission map estimation using a fuzzy inference system.

3.3. Estimation of atmospheric light

Because atmospheric light is incident on atmospheric particles, it is scattered. For the hazy image model in Eq. (1), if the transmission map approaches 0, the hazy image will be equal to the color vector of atmospheric light. Therefore, the sky or a white area in the image is often selected as the reference for estimating atmospheric light. A higher or lower estimated value of atmospheric light will yield a dim or bright dehazed image, respectively. Thus, it is difficult to obtain an accurate value of atmospheric light from a hazy image. Narasimhan and Nayar [6] considered the vanishing point interaction in an image as atmospheric light. Because this method does not determine the position of the vanishing point, it is not reliable. Tan [14] selected the brightest pixel from a hazy image for estimating atmospheric light. However, this method has several drawbacks; for example, the brightest pixel may be a white car or a white building. Shiau [18] considered that atmospheric light should not be limited to bright areas. Thus, atmospheric light can be obtained using the weighting ratios of the brightest pixels in bright and the dark regions. In general, atmospheric light is obtained by referring to the method given by He et al. [16], according to which the 0.1% brightest pixels are extracted using a dark channel. Although this method [16] can be used to accurately estimate atmospheric light, it would be difficult to perform dehazing under a few conditions. For example, when the original image contains a nonsky or hazy region (Figure 8a), a large or small patch will be used in the dark channel method. If a large patch is adopted, other lights will be ignored. Therefore, the atmospheric light cannot be estimated.

To overcome the aforementioned problems, an automatic atmospheric light estimation method is presented in this study. First, the minimum pixel values of each pixel in the image across the three color channels are extracted. Next, the 1% highest pixel values are obtained from the image. Then, the obtained pixels are respectively mapped to the pixel positions in the original hazy image. Finally, the pixel values of the three color channels at the acquired pixel positions are respectively summed and divided by 1% of the total number of pixels to obtain the final color vector of atmospheric light. The pseudocode of the estimated atmospheric light is shown in Table 1. This approach involves extracting the minimum pixel value of each pixel in the entire image. If there is no sky area in the image, atmospheric light is estimated from white areas in the image. Thus, white areas can be considered a part of the atmospheric light. The estimated atmospheric light in this study is shown in Figure 8b.

Table 1. Atmospheric light estimation algorithm.

1:	$I_{gray}(x) = \min(I_c(x))$
2:	counter = Width of image* Height of image *1%
3:	for (pixel value Descending from 255 to 0)
4:	for (Width of image)
5:	for (Height of image)
6:	if ($I_{gray}(x) ==$ current Index of pixel value)
7:	pixel _c (x)+ = $I_c(x)$, counter --
8:	end if
9:	end for
10:	end for
11:	end for
12:	$A_c = \frac{\text{pixel}_c(x)}{\text{Width*Height*1\%}}$



Figure 8. a) Haze image, b) the atmospheric light position.

3.4. Image restoration

When both atmospheric light A_c and transmission $t_{ref}(x)$ are given, image restoration is performed as follows:

$$J_c(x) = \frac{I_c(x) - A_c}{t_{ref}(x)} + A_c. \quad (6)$$

4. Experimental results

In this study, experiments are divided into qualitative and quantitative assessments. Qualitative assessment is visual assessment, whereas quantitative assessment is based on the visibility quantitative assessment of the restored image.

4.1. Visual assessment

In this experiment, four original hazy images, called “ny12”, “ny17”, “y01”, and “y16”, were used for analysis and evaluation. We compared our method with the methods proposed by Fattal [13], Tan [14], Kopf et al. [7], Tarel et al. [15], and He et al. [16]. The visual assessment considered overbrightness, color shift, color oversaturation, halo, white spots, and sharp edges. Detailed experimental results of various methods are shown in Tables 2 and 3.

The haze in original images can be seen on buildings and mountains. In images obtained using Fattal’s [13] method, the sky is excessively bright in the backgrounds of images “ny12” and “y16.” In images obtained using Tan’s [14] method, the problem of color shift is apparent in the building and sky in the dehazed version of the image “ny12.” In addition, the strong contrast in images “y17,” “y01,” and “y16” causes color oversaturation, and a halo appears on the edge of the rock in “y16.” In images obtained using the method of Kopf et al. [7], color oversaturation can be seen in a few areas of the building and sky in image “ny12” and in the foreground buildings in image “ny17.” Moreover, color shift can be seen in images “y01” and “y16.” In images obtained using the method of Tarel et al. [15], color oversaturation can be seen in the sky region, and a halo can be seen on the edges of buildings and mountains. In images obtained using the method of He et al. [16], excessive color shifts and color oversaturation can be observed, which makes the images look unnatural.

Thanks to the fact that more appropriate atmospheric light is obtained in the proposed method, the dehazing results of “ny12” and “ny17” do not lose the original colors in the sky, have a gradient of color in the foreground building, and show quite natural in the distant buildings. For the images “y01” and “y16”, the dehazed images obtained using the proposed method show the same color in the sky region as that in the original image, and the details of the mountains are clearly visible. The result is satisfactory.

Table 2. Disadvantages of various methods.

	Methods	Fattal [13]	Tan [14]	Kopf et al. [7]	Tarel et al [15]	He et al. [16]
	Images					
ny12	over bright color shift color oversaturation halo white spots	✓	✓	✓	✓ ✓	✓
ny17	over bright color shift color oversaturation white spots white spots		✓	✓	✓ ✓	✓
y01	over bright color shift color oversaturation halo sharp edges		✓	✓	✓ ✓	✓
y16	over bright color shift color oversaturation halo sharp edges	✓	✓ ✓	✓	✓ ✓	✓ ✓

















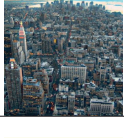
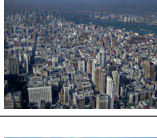


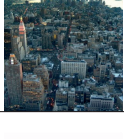
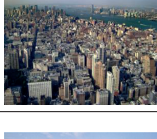
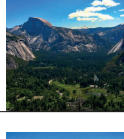
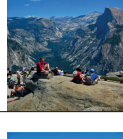


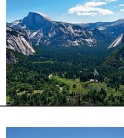
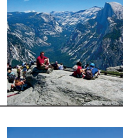
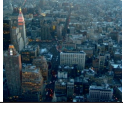

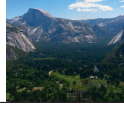
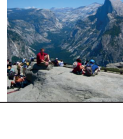
4.2. Quantitative evaluation

The quantitative evaluation of image restoration is a difficult task, and no uniform standard is available for this purpose. Therefore, in this study, the S-CIELAB color difference metric proposed by Zhang and Wandell [26] is proposed. This method is for the original image and reconstructed image in each single color block for difference evaluation. The experimental results are compared with those of other methods [7, 13–16]. Table 4 lists the various results obtained using the S-CIELAB color difference metric. The experimental results show that the proposed method is superior to other methods according to the S-CIELAB color difference metric, and the edges of the restored images do not show color oversaturation.

5. Conclusion

An effective dehazing method was presented in this paper based on the attenuation of light to estimate the transmission map by using a fuzzy inference system. To solve the color oversaturation problem by using a nonlinear quadratic function to refine the transmission map, the color vector of atmospheric light was estimated using the 1% brightest region. Finally, the transmission map and atmospheric light were obtained to reconstruct

Table 3. The results of comparison of various methods.

Methods Images	ny12	ny17	y01	y16
Original image				
Fattal [13]				
Tan [14]				
Kopf et al. [7]				
Tarel et al. [15]				
He et al. [16]				
Liu et al. [20]				
Proposed method				

the image. Experiments were divided into qualitative and quantitative assessments. Qualitative assessment is visual assessment, whereas quantitative assessment is based on the visibility quantitative assessment of the restored image. Experimental results demonstrated that this method is effective and provides good color contrast and visibility.

Table 4. Estimation of color difference using various methods.

Methods \ Images	ny12	ny17	y01	y16
	Fattal [13]	20,993	15,997	2683
Tan [14]	39,394	43,478	15,651	10,244
Kopf et al. [7]	10,096	3853	5891	4012
Tarel et al. [15]	1315	1299	499	3066
He et al. [16]	1462	1357	511	6496
Proposed method	1879	345	179	1556

Acknowledgment

The authors would like to thank the Ministry of Science and Technology of the Republic of China, Taiwan, for financially supporting this research under Contract No. MOST 106-2221-E-167-016.

References

- [1] Pan X, Xie F, Jiang Z, Yin J. Haze removal for a single remote sensing image based on deformed haze imaging model. *IEEE SIGNAL PROC LET* 2015; 22: 1806-1810.
- [2] Ni W, Gao X, Wang Y. Single satellite image dehazing via linear intensity transformation and local property analysis. *Neurocomputing* 2016; 175: 25-39.
- [3] Huang Y, Ding W, Li H. Haze removal for UAV reconnaissance images using layered scattering model. *Chinese Journal of Aeronautics* 2016; 29: 502-511.
- [4] Huang SC, Chen BH, Wang WJ. An efficient visibility enhancement algorithm for road scenes captured by intelligent transportation systems. *IEEE Trans on Intelligent Transportation Systems* 2014; 15: 2321-2332.
- [5] Tan K, Oakley JP. Enhancement of color images in poor visibility conditions. *Proceedings 2000 International Conference on Image Processing*. Vancouver, British Columbia, Canada: IEEE; 2000. pp. 788-791.
- [6] Narasimhan SG, Nayar SK. Interactive (De) weathering of an image using physical models. *IEEE Workshop on Color and Photometric Method in Computer Vision*. New York, NY, USA: IEEE; 2003. pp. 1387-1394.
- [7] Kopf J, Neubert B, Chen B, Cohen M, Cohen-Or D, Deussen O, Uyttendaele M, Lischinski D. Deep photo: model-based photo graph enhancement and viewing. *ACM Trans. Graphics* 2008; 27: 116:1-116:10.
- [8] Schechner YY, Narasimhan SG, Nayar SK. Polarization based vision through haze. *APPL OPTICS* 2003; 42: 511-525.
- [9] Shwartz S, Namer E, Schechner YY. Blind haze separation. *Proceedings of the 2006 IEEE Computer Society Conference on Computer Vision and Pattern Recognition (CVPR'06)*. New York, NY, USA: IEEE; 2006. pp. 1984-1991.
- [10] Narasimhan SG, Nayar SK. Chromatic framework for vision in bad weather. *Proceedings of the 2000 IEEE Conference on Computer Vision and Pattern Recognition*. Vancouver, Canada: IEEE; 2000. pp. 598-605.
- [11] Narasimhan SG, Nayar SK. Vision and the atmosphere. *International Journal of Computer Vision* 2002; 48: 233-254.
- [12] Nayar SK, Narasimhan SG. Vision in bad weather. *Proceedings of the 1999 Seventh IEEE International Conference on Computer Vision*. Kerkyra, Corfu, Greece: IEEE; 1999. pp. 820-827.
- [13] Fattal R. Single image dehazing. *Proceedings of ACM SIGGRAPH* 2008; 27: 1-8.
- [14] Tan RT. Visibility in bad weather from a single image. *Proceedings of the 2008 IEEE Conference on Computer Vision and Pattern Recognition*. Anchorage, Alaska: IEEE; 2008. pp. 1-8.

- [15] Tarel JP, Hautiere N. Fast visibility restoration from a single color or gray level image. Proceedings of the 2009 IEEE 12th International Conference on Computer Vision. Kyoto, Japan: IEEE; 2009. 2201-2208.
- [16] He K, Sun J, Tang X. Single image haze removal using dark channel prior. IEEE Transactions on Pattern Analysis and Machine Intelligence 2011; 33: 2341-2353.
- [17] He K, Sun J, Tang X. Guided image filtering. IEEE Trans on Pattern Analysis and Machine Intelligence 2013; 35:1397-1409.
- [18] Shiau YH, Chen PY, Yang HY, Chen CH, Wang SS. Weighted haze removal method with halo prevention. J VIS COMMUN IMAGE R 2014; 25: 445-453.
- [19] Ancuti CO, Ancuti C. Single image dehazing by multi-scale fusion. IEEE T IMAGE PROCESS 2013; 22: 3271-3282.
- [20] Ge GY, Wei ZZ, Zhao JX. Fast single-image dehazing using linear transformation. OPTIK 2015; 126: 3245-3252.
- [21] Wang JG, Tai SC, Lin CJ. Image haze removal using a hybrid of fuzzy Inference system and weighted estimation. J ELECTRON IMAGING 2105; 24: 033027-1-033027-13.
- [22] Zadeh LA. Fuzzy sets. INFORM CONTROL 1965; 8: 338-353.
- [23] Van TL, Nguyen TH, Lee DC. Advanced pitch angle control based on fuzzy logic for variable-speed wind turbine systems. IEEE Lat Am T 2015; 30: 578-587.
- [24] Ruelas EA, Vazquez JA, Yanez J, Lopez I, Bravo CF. Condition estimation of carbon steel using a neuro-fuzzy system and image processing. IEEE Lat Am T 2015; 13: 2322-2328.
- [25] Mahapatra A, Mishra TK, Sa PK, Majhi B. Background subtraction and human detection in outdoor videos using fuzzy logic. In: IEEE 2013 International Conference on Fuzzy Systems. Hyderabad, India. New York, NY, USA: IEEE; 2013. pp. 1-7.
- [26] Zhang X, Wandell BA. Color image fidelity metrics evaluated using image distortion maps. SIGNAL PROCESS 1998; 7: 201-214.